Re-assessing copper and nickel enrichments as paleo-productivity proxies

Nicolas Tribovillard

BSGF - Earth Sciences Bulletin 2021, 192, 54
© N. Tribovillard, Published by EDP Sciences 2021
https://doi.org/10.1051/bsgf/2021047

BSGF
Earth Sciences Bulletin
Available online at:
www.bsgf.fr

Re-assessing copper and nickel enrichments as paleo-productivity proxies

Nicolas Tribovillard*

Univ. Lille, CNRS, Univ. Littoral Côte d'Opale, UMR 8187 – LOG – Laboratoire d'Océanologie et de Géosciences, F-59000 Lille, France

Received: 8 September 2020 / Accepted: 6 October 2021 / Publishing online: 3 November 2021

Abstract – Copper (Cu) and nickel (Ni) are elements frequently enriched in sedimentary deposits rich in organic matter (OM). In the marine environment, they are mainly supplied to the sediments in association with sedimentary OM (organo-metal complexes). In modern environments, a good correlation between the intensity of phytoplankton productivity and the quantities of Cu and Ni transferred to sediments made it possible to establish paleo-productivity calculations based on the contents of ancient sediments in these two metals. The present study is a re-evaluation of the significance that can be attributed to these two metals as paleo-productivity proxies. The approach adopted here is based on the examination of a large database already available in the scientific literature. The choice was made to favor the examination of a large amount of data by simple means: comparisons of total organic carbon (TOC) content, enrichment in Cu and Ni (or even other trace metals), and value of the Fe:Al ratio that makes it possible to assess the availability of reactive iron. The basic idea is that the examination of a large number of geological formations makes it possible to encompass all kinds of paleo-environmental settings, thus comprising an extreme range of the factors conventionally involved in the mechanisms of accumulation of OM. The aim is to identify strong trends, valid in a large number of paleo-situations, which will have to be carefully taken into account in future detailed paleo-environmental reconstructions. It emerges from this study that, in many cases, Cu and Ni cannot be considered as faithfully reflecting the quantity of OM initially deposited. Several factors acting on the loss of Cu and Ni can be identified, among them, (1) a rapid loss linked to the decomposition of the OM before the conditions conducive to sulfate-reduction set in; (2) a low abundance of reactive iron which limits the quantity of pyrite liable to form, which significantly hampers Cu and Ni fixation in sediments. If Cu and Ni are not reliably retained in the sediments, that is, proportional to the quantity of OM supplied to the sediment, the paleo-environmental reconstitutions involving the concentrations of these metals may provide underestimated values of paleoproductivity. An interesting clue is the Fe:Al ratio that makes it possible to quickly know whether the values of the Cu and Ni enrichments are likely to be "abnormally" low.

Keywords: marine sediments / trace metals / paleo-environmental reconstructions / organic matter / enrichment factors / reactive iron availability

Résumé – Ré-évaluation des enrichissements en cuivre et en nickel comme marqueurs de paléo-productivité. Le cuivre (Cu) et le nickel (Ni) sont des éléments fréquemment enrichis dans les dépôts sédimentaires riches en matière organique (MO). Dans le milieu marin, ils sont principalement apportés aux sédiments en association avec la MO sédimentaire. Dans les environnements actuels, une bonne corrélation entre l'intensité de la productivité phytoplanctonique et les quantités de Cu et Ni transférées aux sédiments a permis d'établir des calculs de paléoproductivité reposant sur les teneurs des sédiments anciens en ces deux métaux. La présente étude est une ré-évaluation de la valeur qui peut être attribuée à ces deux métaux en tant que traceurs de paléoproductivité. L'approche adoptée ici repose sur l'examen d'une base de données volumineuse déjà accessible dans la littérature scientifique. Le choix fut fait de privilégier l'examen d'un grand nombre de données par des moyens simples : des comparaisons des teneurs en carbone organic total (TOC), des enrichissement en Cu et Ni (voire d'autres métaux traces), et des valeurs du rapport Fe:Al qui permet d'apprécier la disponibilité du fer réactif. L'idée de base est que l'examen d'un grand nombre de formations géologiques (grâce à cette vaste base de données) permet d'englober toutes sortes de situations

*Corresponding author: nicolas.tribovillard@univ-lille1.fr

paléoenvironnementales comprenant donc une extrême variété des facteurs classiquement impliqués dans les mécanismes d'accumulation de MO. Le but est de dégager des tendances fortes, valables dans un grand nombre de paléosituations, qui devront être soigneusement pris en compte, à l'avenir, dans les reconstitutions paléoenvironnementales détaillées. Il ressort de cette étude que, dans de nombreux cas, le Cu et le Ni ne peuvent pas être considérés comme reflétant fidèlement la quantité de MO initialement déposée. Plusieurs facteurs agissant sur la perte de Cu et Ni peuvent être mis en avant, et parmi eux, (1) une perte rapide liée à la décomposition de la MO avant que les conditions propices à la réduction des sulfates ne s'installent ; (2) une faible abondance de fer réactif qui limite la quantité de pyrite susceptible de se former, ce qui entrave la fixation de Cu et Ni dans les sédiments. Si Cu et Ni ne sont pas retenus de manière fidèle dans les sédiments, c'est-à-dire proportionnelle à la quantité de MO transférée au sédiment, les reconstitutions paléoenvironnementales impliquant les concentrations de ces métaux peuvent fournir des valeurs sous-estimées pour la paléoproductivité. Un indice intéressant est le rapport Fe:Al qui permet de savoir rapidement si les valeurs des enrichissements en Cu et Ni sont susceptibles d'être « anormalement » basses.

Mots clés : sédiments marins / éléments traces / reconstructions paléo-environnementales / matière organique / facteurs d'enrichissement / disponibilité en fer réactif

1 Introduction

Assessing paleoproductivity has always been an important point for paleoenvironmental reconstructions. However, paleoproductivity is not easy to track back because many phenomena may hamper or alter its record, during deposition and (early) diagenesis of sediments (*e.g.*, Burdige, 2006; Steiner *et al.*, 2017 and references therein). Various approaches have been established, based on the organic content of the sediments and/or their inorganic geochemistry. Productivity, organic matter flux to the sediment and total organic carbon content in the sediments are three distinct parameters. Even in modern environments it is challenging to predict the relationship between them without additional indications such as latitude, water depth, oxygen levels in the water column, to mention a few. The use of the organic matter content of the sediment as a proxy for paleo-productivity is possibly more questionable than the use of the metals.

This study proposes to examine relationships between the organic content of sedimentary rocks – measured by their content in total organic carbon or TOC – and their enrichment in copper (Cu) and nickel (Ni) in order to assess the value of the enrichment in these two metals as paleo-productivity proxies. To reconstruct the paleo-productivities as well as possible, the conditions of organic matter (OM) preservation and dilution are necessarily taken into consideration. These preservation conditions are linked to many factors, beyond just the redox conditions. It is therefore necessary to be able to embrace all of the paleo-environmental factors prevailing at the time of sediment deposition and early diagenesis. However, these factors are often interdependent, which further complicates paleo-environmental reconstructions, and, ultimately, each paleo-situation is, too often, a unique case, requiring a careful examination of local factors as well as larger-scale ones.

In this paper, to test the relationships between TOC and Ni and Cu enrichments, a diametrically opposite approach is proposed. Rather than examining in detail a limited number of cases, the choice was made to increase considerably the number of study cases. Taking into account a large number of geological formations and, thus, a very large number of samples makes it possible to multiply and therefore to mix diverse sedimentary conditions. We can thus gather, in the same database, situations under contrasted conditions of seawater oxygenation, water-column stratification and hydrodynamism, surface productivity (nature and intensity), sedimentation rates, grain-size distribution and mineralogical or chemical composition of the sediment particles, bioturbation and bio-irrigation, to mention the classically evoked parameters. Mixing all these contexts in the same database will allow major trends to be highlighted, being valid for a large array of depositional settings, as will be discussed in this paper.

2 Materials and methods

We used, thanks to the professional courtesy of Thomas J. Algeo, the database studied by Algeo and Liu (2020); the database is available on line as supplementary material accompanying their paper (https://doi.org/10.1016/j.chemgeo.2020.119549). We also took advantage of the information and advice on use that T.J. Algeo kindly provided.

The database consists of 55 elemental geochemical datasets for Phanerozoic marine units spanning the Cambrian to Recent (Tab. 1 + supplemental references). The total number of analyzed samples is 5143. Collectively, the database includes examples of all major redox facies ranging from oxic to euxinic. The study formations are all argillaceous, ranging from gray shales and marls for the oxic facies to black shales for the anoxic ones. For their study, Algeo and Liu (2020) tabulated the same suite of elemental redox proxies for all 55 study formations. This suite included a total of 21 proxies; for the present study, the following proxies have been considered: TOC, Fe:Al, Cu-EF, Mo-EF, Ni-EF and U-EF, where EF stands for enrichment factor. Enrichment factors (EF) were calculated as: $X\text{-}EF = [(X:Al)_{sample}/(X:Al)_{upper\ crust}]$, where X and Al represent the concentrations of element X and Al, respectively (weight %). Samples were normalized using the average composition of the Earth's upper crust after McLennan (2001). This reference was chosen by Algeo and Liu (2020) because it is widely used. Thus, the values used for EF calculation are the followings, expressed in weight percents or ppm: Al, 8.04%, Fe, 3.50%, Cu, 25 ppm and Ni, 44 ppm. Consequently, the Fe/Al ratios are also expressed in mass/mass.

Table 1. List of the formations studied, with the location and age indicated, together with the references where the data come from. The papers corresponding specifically to Table 1 are listed at the end of the reference list (supplemental references).

N°	Formations	Location (section/core)	Age	Redox status	Sources
1	Kacak Beds	Mech Irdane, Morocco	Mid Devonian	oxic	Ellwood *et al.* (2011) Palaeo-3, 304(1-2), 74–84.
2	Kamura Fm	Kamura, Japan	Early Triassic	oxic	Zhang *et al.* (2019) Palaeo-3, 519, 65–83.
3	Gerennavar Fm	Balvany, Hungary	Early Triassic	oxic	Schobben *et al.* (2017) Palaeo-3, 486, 74–85.
4	Dong Dang Fm	Lung Cam, Vietnam	Early Triassic	oxic	Algeo (unpubl. data); *cf.* Son *et al.* (2007) Palaeoworld 16(1-3), 51–66; Wardlaw *et al.* (2015) Micropaleont. 61(4), 313–334.
5	Modern sediments	East Philippine Sea (WPD-03)	Quaternary	oxic	Xiong *et al.* (2012) Chem. Geol. 334, 77–91.
6	Dalong-Luolou Fms	Taiping, South China	Early Triassic	oxic	Algeo (unpubl. data); *cf.* Krull *et al.* (2004) Palaeo-3, 204(3-4), 297–315; Luo *et al.* (2011) Palaeo-3, 299(1-2), 70–82.
7	Dalong-Luolou Fms	Daxiakou, South China	Early Triassic	oxic-dysoxic	Shen *et al.* (2012) Geology 40(11), 963–966; Shen *et al.* (2013) J. Asian Earth Sci 75, 95–109.
8	Hushpuckney Shale	Kansas, USA (Ermal)	Late Pennsylvanian	dysoxic	Hoffman *et al.* (1998), in Shales and Mudstones (J. Schieber *et al.*, eds.), vol. 1, pp. 243–269.
9	Modern sediments	Black Sea (Unit 3)	Holocene	dysoxic-euxinic	Algeo and Li (2020), Geochim. Cosmochim. Acta, in press.
10	Missourian Stage	Iowa, USA (Logan)	Late Pennsylvanian	oxic-dysoxic	Algeo (unpubl. data).
11	Pelagic PTB shales	Gujo-Hachiman, Japan	Early Triassic	dysoxic	Algeo *et al.* (2010) Geology 38(2), 187–190; Algeo *et al.* (2011) Palaeo-3, 308(1-2), 65–83.
12	Ursula Creek	Ursula Creek, B.C., Canada	Early Triassic	dysoxic-euxinic	Algeo (unpubl. data); *cf.* Henderson (1997) Bull Can. Petrol. Geol. 45 (4), 693–707; Wignall and Newton (2003) Palaios 18(2), 153–167.
13	Hanover-Dunkirk Shales	New York, USA (West Valley)	Late Devonian	dysoxic-euxinic	Algeo (unpubl. data); *cf.* Murphy *et al.* (2000) Geology 28(5), 427–430; Sageman *et al.* (2003) Chem. Geol. 194(1-4) 229–273; Ver Straeten *et al.* (2011) Palaeo-3, 304(1-2), 54–73.
14	Sulphur Mtn Fm	Opal Creek, Alberta, Canada	Early Triassic	euxinic	Schoepfer *et al.* (2013) GPC 105, 21–35.
15	Modern sediments	California Margin (ODP 167)	Quaternary	oxic-dysoxic	Tada *et al.* (2000) Proc. ODP Sci. Res. 167, 277–296; Irino and Pedersen (2000) Proc. ODP Sci. Res. 167, 263–271.
16	Llanvirn-Llandeilo shales	Aberystwyth Bay, Wales, UK	Mid Ordovician	dysoxic	Lev (1994) M.S. Thesis, Univ. Cincinnati.
17	Excello Shale	Kansas, USA (Edmonds)	Mid Pennsylvanian	euxinic	Herrmann *et al.* (2019) Palaeo-3, 109235.
18	Modern sediments	Saanich Inlet, B.C., Canada	Holocene	dysoxic-euxinic	François (1987) Ph.D. Dissertation, Univ. British Columbia.
19	Heather Fm	North Sea	Late Jurassic	dysoxic	Jones (1991) Ph.D. Dissertation, Univ. Newcastle upon Tyne; Jones and Manning (1994) Chem. Geol. 111, 111–129.
20	Modern sediments	Black Sea	Holocene	euxinic	Lyons (1992) Ph.D. Dissertation, Yale University.
21	Kennecott Point Fm	British Columbia, Canada	Triassic–Jurassic boundary	dysoxic-euxinic	Schoepfer *et al.* (2016) EPSL 451, 138–148.
22	Modern sediments	Cariaco Basin, Venezuelan Shelf	Holocene	dysoxic-euxinic	Lyons *et al.* (2003) Chem. Geol. 195(1), 131–157.
23	Wufeng-Longmaxi Shales	Jiaoye, South China	Ordovician-Silurian	euxinic	Shen *et al.* (2019) EPSL 511, 130–140.
24	Missourian Stage	Kansas (Edmonds)	Late Pennsylvanian	oxic-dysoxic	Algeo (unpubl. data); *cf.* Algeo *et al.* (2004) Chem. Geol. 206(3-4), 259–288.
25	Modern sediments	Black Sea (Stn 6)	Holocene	euxinic	Lüschen (2004) Ph.D. Dissertation, Univ. Oldenburg.
26	modern sediments	Black Sea	Holocene	euxinic	Brumsack (1989) Geol. Rundschau. 78(3), 851–882.
27	Wufeng-Longmaxi Shales	Yanzhi, South China	Ordovician-Silurian	euxinic	Shen *et al.* (2019) EPSL 511, 130–140.
28	Kimmeridge Fm	North Sea	Late Jurassic	euxinic	Jones (1991) Ph.D. Dissertation, Univ. Newcastle upon Tyne; Jones and Manning (1994) Chem. Geol. 111, 111–129.
29	Wufeng-Longmaxi Shales	Qiliao, South China	Ordovician-Silurian	euxinic	Shen *et al.* (2019) EPSL 511, 130–140.

Table 1. (continued).

N°	Formations	Location (section/core)	Age	Redox status	Sources
30	Three Lick Bed	Kentucky, USA	Late Devonian	euxinic	Robl and Barron (1988) in Devonian of the World, vol. II, pp. 377–392.
31	Lansing Fm	New York, USA	Mid Devonian	euxinic	Algeo (unpubl. data); *cf.* Brett *et al.* (2011) Palaeo-3, 304(1-2), 21–53; DeSantis and Brett (2011) Palaeo-3, 304(1-2), 113–135.
32	Draupne Fm	North Sea	Late Jurassic	euxinic	Jones (1991) Ph.D. Dissertation, Univ. Newcastle upon Tyne; Jones and Manning (1994) Chem. Geol. 111, 111–129.
33	Upper Huron Shale	Kentucky, USA	Late Devonian	euxinic	Robl and Barron (1988) in Devonian of the World, vol. II, pp. 377–392.
34	Middle Huron Shale	Kentucky, USA	Late Devonian	euxinic	Robl and Barron (1988) in Devonian of the World, vol. II, pp. 377–392.
35	modern sediments	Cariaco Basin, Venezuelan Shelf	Holocene	dysoxic-euxinic	Piper and Dean (2002) USGS Prof Pap 1670.
36	Cleveland Shale	Ohio, USA (OHDW)	Late Devonian	euxinic	Jaminski (1998) Ph.D. Dissertation, Univ. Cincinnati; Jaminski *et al.* (1998) in Shales and Mudstones (J. Schieber *et al.*, eds.), vol. 1, pp. 217–242.
37	Lower Huron Shale	Kentucky, USA	Late Devonian	euxinic	Robl and Barron (1988) in Devonian of the World, vol. II, pp. 377–392.
38	Excello Shale	Iowa, USA (Logan)	Mid Pennsylvanian	euxinic	Herrmann *et al.* (2019) Palaeo-3, 109235.
39	Woodford Shale	Oklahoma and Texas, USA	Late Devonian	euxinic	Algeo and Tribovillard (2009) Chem. Geol. 268(3-4), 211–225.
40	Heebner Shale	Kansas, USA (Heinen)	Late Pennsylvanian	euxinic	Turner *et al.* (2019) Palaeo-3, 531, 109023.
41	Tacket Shale	Oklahoma, USA (CTW-1)	Late Pennsylvanian	dysoxic-euxinic	Algeo *et al.* (2004) Chem. Geol. 206(3-4), 259–288; *cf.* Cruse and Lyons (2004) Chem. Geol. 206(3-4), 319–345.
42	Sunbury Shale	Ohio, USA (OHRS)	Early Mississippian	euxinic	Jaminski (1998) Ph.D. Dissertation, Univ. Cincinnati; Jaminski *et al.* (1998) in Shales and Mudstones (J. Schieber *et al.*, eds.), vol. 1, pp. 217–242.
43	Cleveland Shale	Ohio, USA (OHRS)	Late Devonian	euxinic	Jaminski (1998) Ph.D. Dissertation, Univ. Cincinnati; Jaminski *et al.* (1998) in Shales and Mudstones (J. Schieber *et al.*, eds.), vol. 1, pp. 217–242.
44	Modern sediments	Black Sea (Stn 7)	Holocene	euxinic	Lüschen (2004) Ph.D. Dissertation, Univ. Oldenburg.
45	Chattanooga Shale	Tennessee, USA	Late Devonian	euxinic	Over *et al.* (2019) Palaeo-3, 524, 137–149; Song *et al.* (2020) GSA Bull., in review.
46	Hushpuckney Shale	Kansas, USA (Womelsdorf)	Late Pennsylvanian	euxinic	Algeo *et al.* (2004) Chem. Geol. 206(3-4), 259–288.
47	Stark Shale	Kansas, USA (Womelsdorf)	Late Pennsylvanian	euxinic	Algeo (unpubl. data); *cf.* Hatch and Leventhal (1992) Chem. Geol. 99 (1-3), 65–82.
48	Cleveland Shale	Kentucky, USA	Late Devonian	euxinic	Robl and Barron (1988) in Devonian of the World, vol. II, pp. 377–392.
49	Heebner Shale	Iowa, USA (Riverton)	Late Pennsylvanian	euxinic	Turner *et al.* (2019) Palaeo-3, 531, 109023.
50	Cleveland Shale	Kentucky, USA (KEP-3)	Late Devonian	euxinic	Jaminski (1998) Ph.D. Dissertation, Univ. Cincinnati; Jaminski *et al.* (1998) in Shales and Mudstones (J. Schieber *et al.*, eds.), vol. 1, pp. 217–242.
51	Sunbury Shale	Kentucky, USA (KEP-3)	Early Mississippian	euxinic	Jaminski (1998) Ph.D. Dissertation, Univ. Cincinnati; Jaminski *et al.* (1998) in Shales and Mudstones (J. Schieber *et al.*, eds.), vol. 1, pp. 217–242.
52	Hushpuckney Shale	Iowa, USA (Riverton)	Late Pennsylvanian	euxinic	Algeo (unpubl. data); *cf.* Cruse and Lyons (2004) Chem. Geol. 206(3-4), 319–345.
53	Sunbury Shale	Kentucky, USA	Early Mississippian	euxinic	Robl and Barron (1988) in Devonian of the World, vol. II, pp. 377–392.
54	Excello Shale	Kansas, USA (Lafarge Quarry)	Mid Pennsylvanian	euxinic	Herrmann *et al.* (2019) Palaeo-3, 109235.
55	Hushpuckney Shale	Iowa, USA (Logan)	Late Pennsylvanian	euxinic	Algeo (unpubl. data); *cf.* Algeo *et al.* (2004) Chem. Geol. 206(3-4), 259–288.

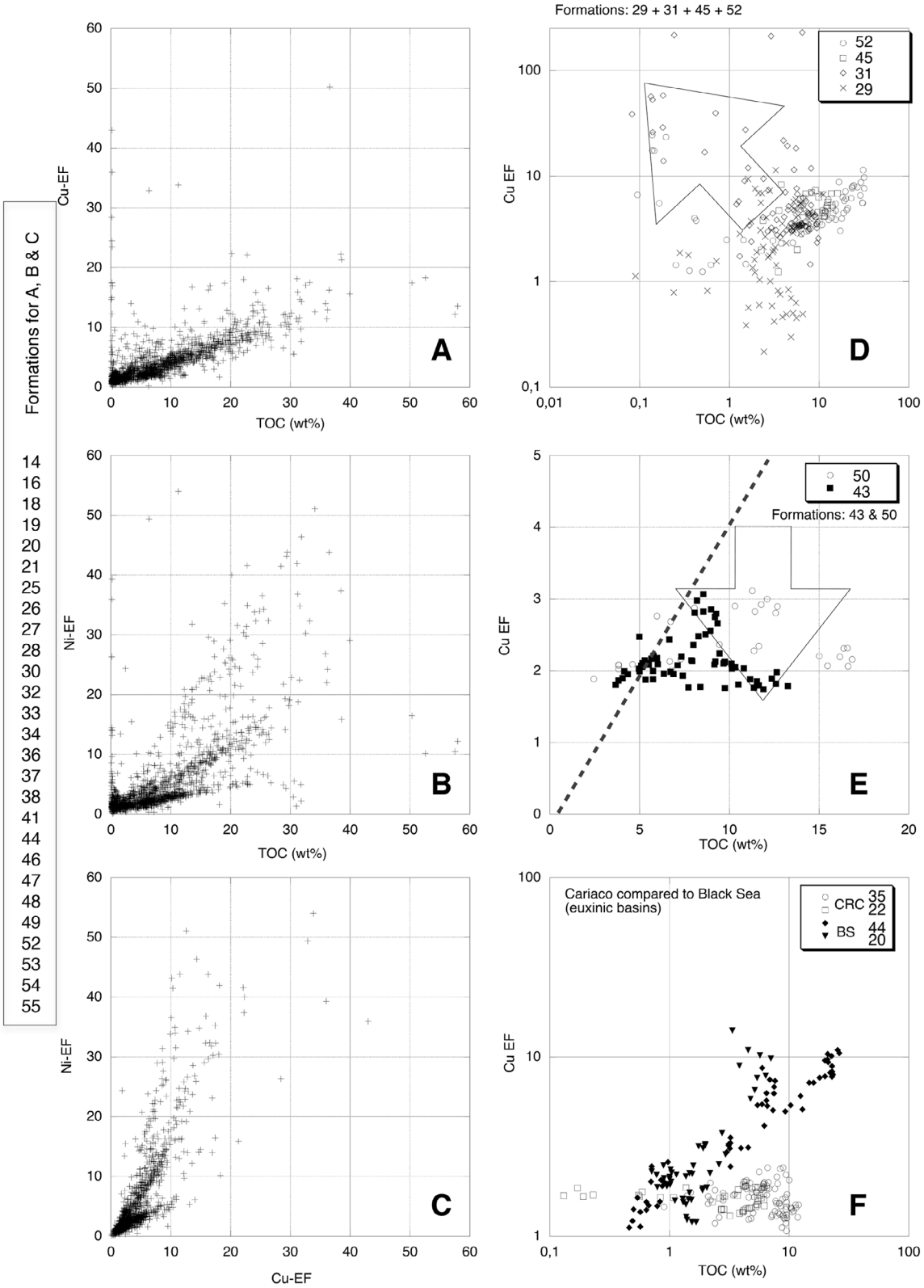

Fig. 1. Relationships between the content in total organic carbon (TOC) and the enrichment factors in copper (Cu-EF, panel A) or nickel (Ni-EF, panel B) for the 27 formations listed on the left-hand side of the figure. The formation names are listed in Table 1. Panel C shows the cross diagram opposing the enrichment factors in Cu and Ni for the same formations. Panel D illustrates the relationships between TOC and Cu-EF for the formations 29, 31, 45 and 52 with samples yielding relative excess in Cu compared to the TOC values (arrow). Panel E: same diagram for formations 43 and 50, showing a relative deficit in Cu compared to the TOC values (arrow). Panel F: same diagram for the samples of two modern euxinic basins, the Cariaco Basin (formations 22 and 35) and the Black Sea (formations 20 and 44).

The common aluminum normalization is used to avoid the effects of variable dilution by carbonate and/or biogenic silica, although certain pitfalls may accompany this approach when aluminum content is minimal (for a discussion, see Van der Weijden, 2002 and Tribovillard *et al.*, 2006). The convenience of using such enrichment factors is that any value larger than 1.0 theoretically points to the enrichment of an element relative to its average crustal abundance. Practically, EFs must be > 3 to be considered as showing a detectable enrichment (for a discussion, see Algeo and Tribovillard, 2009).

Iron has been the focal point of many studies about sediment geochemistry, notably regarding authigenesis and early diagenesis of sediments deposited under reducing conditions. Such conditions are propitious to the formation of iron sulfides and they involve OM. In addition to the seminal papers of Berner (1970, 1984), recent syntheses about iron were written by Raiswell and Canfield (2012), Rickard (2012), Poulton and Canfield (2011), Taylor and Macquaker (2011), Tribovillard *et al.* (2015), Raiswell *et al.* (2018) and Raven *et al.* (2019). In the present paper, with an average crustal value of 0.44 for the Fe:Al ratio (McLennan, 2001), samples with Fe:Al > 0.5 will be considered to be authigenically enriched in iron (discussion in Tribovillard *et al.*, 2015; Raiswell *et al.*, 2018).

3 Results

A first approach consisted in observing the relationships between the content of organic matter (expressed as total organic carbon or TOC) on the one hand, and the enrichment factors of Cu and Ni, on the other hand. Without inclusion of the nine geological formations showing very low TOCs, there is a good correlation between the TOC and copper enrichment factor for 27 geological formations out of 44 ($R^2 = 0.4636$, $N = 2087$; Fig. 1A). A bivariate diagram opposing TOC and Ni enrichment factors (Fig. 1B) also shows correlations but which are more case-specific: several correlation lines emerge while there is only one in the case of copper. Similarly, a bivariate diagram opposing Cu and Ni enrichment factors also shows several correlation lines (Fig. 1C). Thus, for a very large part of the geological formations and of the samples studied, there is a marked relationship between the abundance of organic matter present in sedimentary deposits and the enrichment in copper and nickel.

For a limited number of geological formations, the TOC *versus* Cu-EF cross diagram shows relatively low organic carbon contents despite elevated Cu enrichments (Fig. 1D). Other formations, compared to the general tendency of Figure 1A, show relatively low enrichments in Cu, given the high TOCs (Fig. 1E). Finally, such a bivariate diagram makes it possible to compare two depositional environments exhibiting euxinic conditions, *i.e.*, the Black Sea and the Cariaco Basin (Fig. 1F). If, for the Black Sea samples, the enrichment in Cu is proportional to the organic carbon content, this is not the case at all for the sediments of the Cariaco Basin.

For sedimentary deposits or formations outside the general trend illustrated in Figure 1A, namely, those illustrated in Figures 1D–1F, relationships are examined between the enrichments in Cu and the values of the Fe:Al ratio. It is observed that the samples showing relatively low TOCs compared to their Cu contents (Fig. 1D) have values of the Fe:Al ratio often exceeding the value 0.5 typical of the average composition of the Earth's crust. The values above 0.5 may reach a few tens (Fig. 2A) but the samples showing Fe:Al ratios greater than 10 or Cu-EF greater than 60 will not be taken into account, because such samples show very low aluminum contents, which biases the value of the elemental ratios. Similarly, if we consider the sedimentary deposits with very low TOCs (which bivariate diagrams with TOC are unrevealing), a good correlation links the values of Fe:Al and Cu-EF (Fig. 2B). On the contrary, the samples of Figure 1E, relatively poor in Cu, show low values of the Fe:Al ratio, below the average crustal value (Fig. 2C). Finally, the samples from the Cariaco Basin show a Fe:Al ratio always very close to the crustal value (Fig. 2D). Lastly, all the samples mentioned in Figures 1A–1D show a good correlation between the enrichment factors for Cu and those for Ni (Fig. 2E), which amounts to saying that what has been said for Cu is also valid for Ni.

Finally, it is possible to compare the different geological formations on the basis of the Fe:Al ratio thanks to a box diagram (Fig. 3). This mode of representation makes it possible to highlight the sedimentary deposits for which the median is at a value above the crustal value. These sedimentary formations, shown in Figure 3, are also those for which, on the one hand there are samples relatively poor in TOC compared to enrichment in Cu, and on the other hand, these samples show a correlation between Cu-EF and Fe:Al.

4 Discussion

4.1 Nickel and copper behavior in marine sediment

Nickel and copper are frequently considered together in studies of marine deposits (Plass *et al.*, 2021). Both Ni and Cu may be incorporated into soil OM on land, notably through strong bonds to humic and fulvic acids (*e.g.*, Kördel *et al.*, 1997; Weng *et al.*, 2002; Giacalone *et al.*, 2005). The organometal complexes are transferred to seawater *via* rivers, and marine sediments then collect terrestrial OM that may be rich in Cu and Ni (Jokinen *et al.*, 2020 and references therein). Both Cu and Ni have long been known to be incorporated into marine OM (Sclater *et al.*, 1976; Bruland, 1980; Disnar, 1981; Morel *et al.*, 2003, Bönning *et al.*, 2015, to mention a few).

In oxic marine environments, nickel behaves as a micronutrient being present as soluble Ni^{2+} cations or $NiCl^{+}$ ions but mostly as a soluble carbonate ($NiCO_3$) or adsorbed onto humic and fulvic acids (Calvert and Pedersen, 1993; Whitfield, 2002; Algeo and Maynard, 2004; Ciscato *et al.*, 2018). Complexation of Ni with OM is known to accelerate scavenging in the water column and thus sediment enrichment (Piper and Perkins, 2004; Nameroff *et al.*, 2004; Naimo *et al.*, 2005). Twining *et al.* (2012) showed the active role played by diatom frustules in the transfert of Ni to sediments. Upon OM decay, Ni may be released from organometallic complexes to pore waters. In suboxic sediments, Ni may not trapped within the sediment but cycled from the sediment into the overlying waters because the potential hosting phases, namely, sulfides and Mn oxides, are absent (Tribovillard *et al.*, 2006). Under reducing conditions, Ni may be incorporated as the insoluble sulfide NiS into pyrite as a solid solution; however, the kinetics

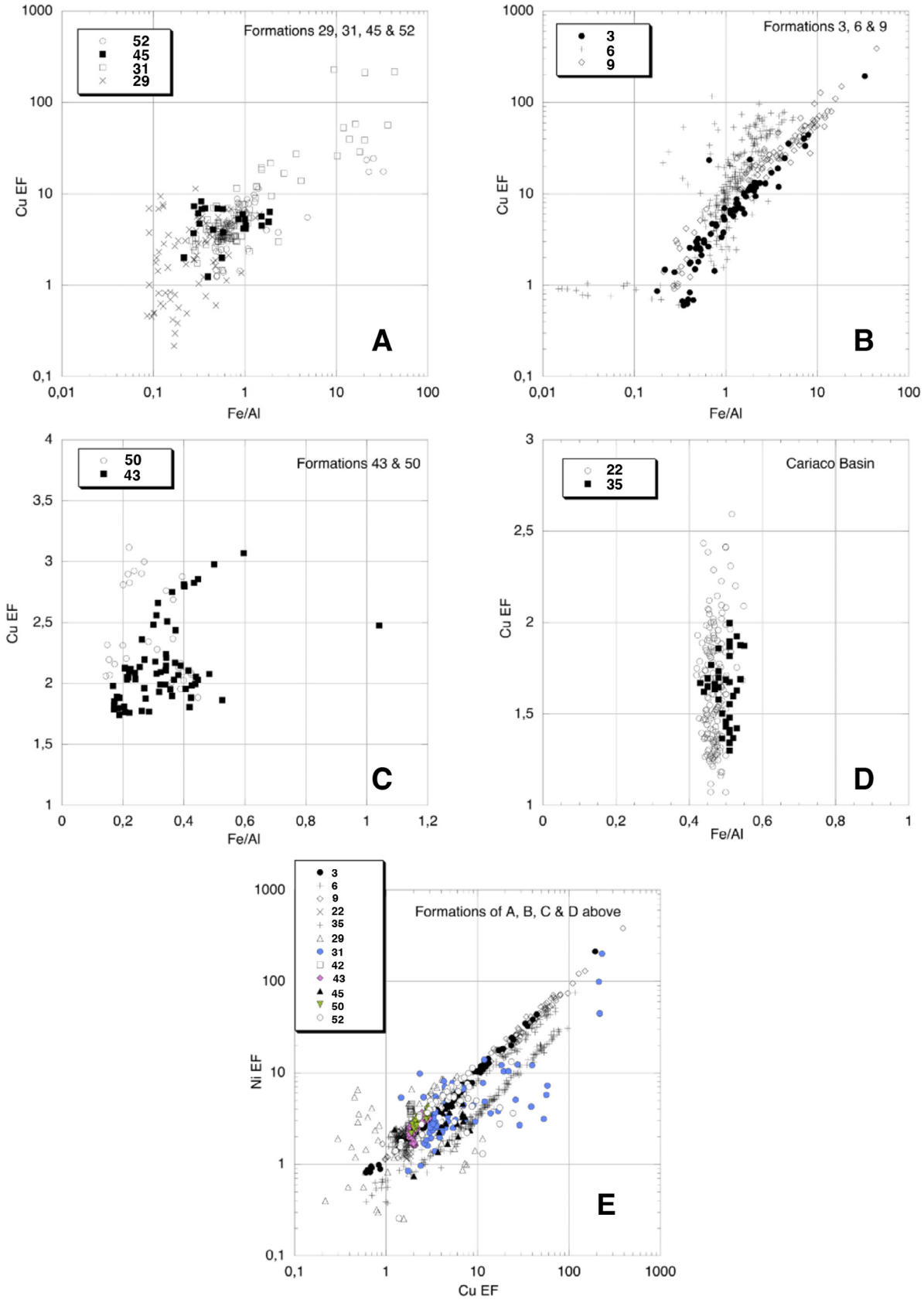

Fig. 2. A to D: diagrams of the relations between the Fe:Al ratio and the enrichment factors in Cu (Cu-EF) for the formations illustrated on the right-hand side of Figure 1. Panel E shows the relations between the enrichment factors in Cu and Ni for all these formations mentioned in panels 2A to 2D. The formation names are listed in Table 1.

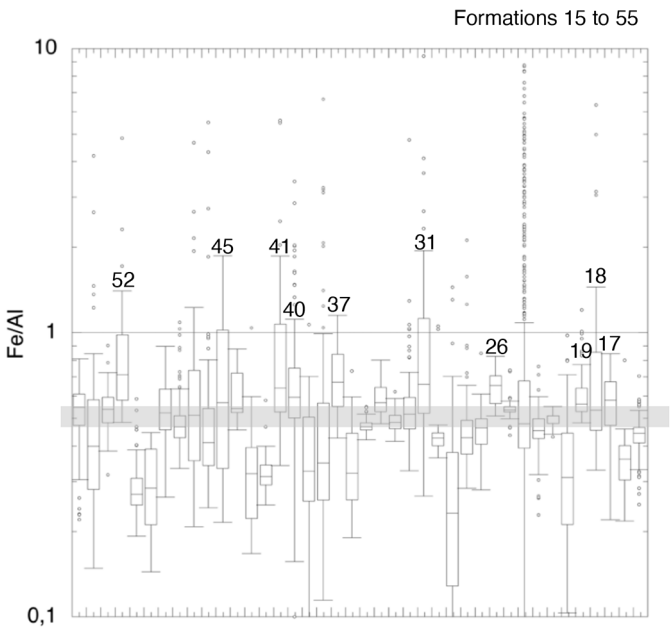

Fig. 3. Box plot for all the formations with a significant TOC content (#15 to 55), illustrating the distribution of the Fe:Al ratio values. Shaded: average crustal value, close to 0.5. The formation names are listed in Table 1.

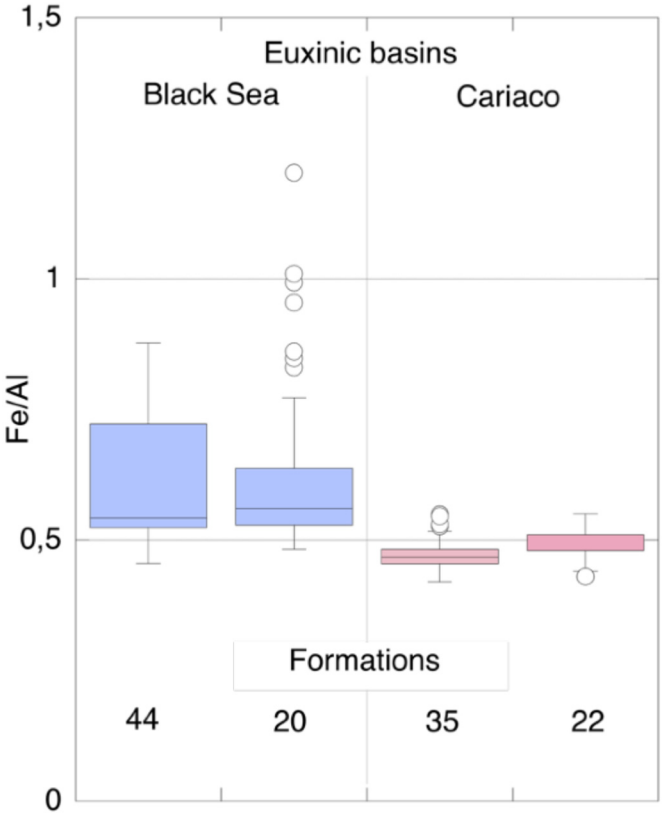

Fig. 4. Box plot of the Fe:Al ratio illustrating the contrasted situations of the Black Sea and the Cariaco Basin. The formation names are listed in Table 1.

of the process are slow (Huerta-Diaz and Morse, 1990, 1992; Morse and Luther, 1999). In the short term, Bönning *et al.* (2015), examining recent sediments deposited below upwelling systems, observed clearcut correlations between Ni and chlorin concentrations, chlorins being immediate degradation products of chlorophyll pigments. In addition, Morin *et al.* (2017) observed the acceleration of pyrite nucleation in the presence of nickel. In the longer term, occasionally, the Ni brought to the sediments by OM may also be incorporated into tetrapyrrole complexes and may be preserved as Ni geoporphyrins under reducing (anoxic/euxinic) conditions (Lewan and Maynard, 1982; Grosjean *et al.*, 2004).

In oxic marine environments, copper is dominantly present as organometallic ligands and, to a lesser extent, dissolved $CuCl^{+}$ ions (Calvert and Pedersen, 1993; Whitfield, 2002; Achterberg *et al.*, 2003; Algeo and Maynard, 2004). Copper behaves only partly as a micronutrient but is also scavenged from solution in deep water (Calvert and Pedersen, 1993). Complexation of Cu with OM, as well as adsorption onto particulate Fe–Mn-oxyhydroxides, will enhance scavenging and sediment enrichment (Fernex *et al.*, 1992; Sun and Püttmann, 2000; Nameroff *et al.*, 2004; Naimo *et al.*, 2005). Through OM remineralization and/or reductive dissolution of Fe–Mn-oxyhydroxides, Cu is released to pore waters. Under reducing conditions, Cu(II) is reduced to Cu(I) and may be incorporated *via* solid solution into pyrite. It may even form its own sulfide phases, CuS and CuS_2 (Huerta-Diaz and Morse, 1990, 1992; Morse and Luther, 1999). In addition, in (hemi-) pelagic sediments with slow sedimentation rates, Cu may be diagenetically fixed by authigenic nontronite or smectite minerals (Pedersen *et al.*, 1986).

There is therefore a strong resemblance, on the whole, between the respective behaviors of Cu and Ni in marine environments since both are mainly brought to sediments by the deposition of OM of terrestrial or marine origin. Some differences can nevertheless be observed between these two metals: Ni remains more easily in solution than Cu in sulfidic waters (Haraldsson and Westerlund, 1988; Bönning *et al.*, 2015; Little *et al.*, 2015) or may be kept within long-lasting, resistant, degradation products of chlorophyl, while Cu is more easily and more quickly incorporated into pyrite during diagenesis (Morse and Luther, 1999; Berner *et al.*, 2013; Large *et al.*, 2014, 2017; Gregory *et al.*, 2015). The reasoning above implicitly means that Cu and Ni are not limited in water masses. Enrichment in trace metals requires that there is a sufficiently large flux of these trace metals to the water body at stake. Higher productivity will not result in sedimentary trace metal enrichment if the metal is depleted in the water column. Similarly, if there is a large increase in the supply of metals (river supply for example), the sediment may get enriched even if production of marine organic matter did not change much. For the ancient sedimentary rocks examined here (except for the Black sea and Cariaco Basin), no such indications are available. In addition, so such reservoir limitation has been mentioned so far in the literature for Ni and Cu, contrary to trace metals that can be massively transferred from the water column to the sediment *via* iron and/or manganeses shuttling; such quantitatively efficient transfer can deplete the water masses in Mo or As (Algeo and Tribovillard, 2009; Tribovillard 2020) but it seems as if Cu and Ni were not concerned (see discussion in Liu and Algeo, 2020).

It is also well known that the degradation of OM in the first stages of diagenesis releases Cu and Ni in a soluble form in interstitial waters, and these metals can then diffuse back to the water column (Chester, 1990; Widerlund, 1996; Charriau *et al.*, 2011; Marchand *et al.*, 2016; Ciscato *et al.*, 2019), or be incorporated into authigenic phases, depending on specific conditions of early diagenesis (François, 1988; Huerta-Diaz and Morse, 1990, 1992; Tribovillard *et al.*, 2006, 2008; Berner *et al.*, 2013).

Lastly, a large number of studies pointed to generally good correlations between the organic-matter content (expressed through TOC values) and Cu and/or Ni concentrations in marine deposits and sedimentary rocks, regardless of the age (within the Phanerozoic) or depositional setting of the marine deposits (Rutten and de Lange, 2003; Algeo and Maynard, 2004; Brumsack, 2006; Piper *et al.*, 2007; Perkins *et al.*, 2008; Tribovillard *et al.*, 2008; Piper and Calvert, 2009; Bönning *et al.*, 2015; Little *et al.*, 2015; Algeo and Liu, 2020). In particular, the overall good correlation of Ni and Cu with TOC suggested to some authors that the main removal mechanism (from seawater) of both metals is settling with OM down to reducing sediments, where Ni would even be more retained within the OM on even longer time-scales (*e.g.*, Algeo and Maynard, 2004, Brumsack, 2006, Piper and Calvert, 2009; Bönning *et al.*, 2015). In addition, Piper and Calvert (2009) used the good relationship observed between TOC and Ni contents to derive paleo-productivity estimates based on Ni accumulation.

4.2 Interpreting correlations between TOC and Ni-Cu

In the present study, we observe a good correlation between the abundance of organic matter (expressed through the TOC) and the enrichment in Cu and Ni in a majority of cases (let us call it situation 1). Thus the enrichment of Cu and Ni is largely proportional to the amount of organic matter actually present in the sedimentary rocks studied. Therefore, if (part of) organic matter has been destroyed and disappeared during diagenesis, the associated Cu and Ni also disappeared from the sediments and the original proportions between OM and the enrichment factors of Cu and Ni have been kept unchanged. It implies that nothing trapped Ni and Cu (no pyrite precipitation) prior a partial departure of these trace metals, as discussed below.

For a limited number of cases, however (situation 2), one can observe formations or subset of samples of some formations with marked Cu and Ni enrichments but relatively low to very low TOC values; one can also identify situations with marked Cu- and Ni-enrichment factors as well as high TOC values, but with TOC relatively low compared to the values that would be expected if the metal enrichments and the TOC were well correlated. In other words, one can detect that OM seems to be (partly) missing in these rocks compared to what might be expected, taking into account significant enrichment in Cu and Ni. In such cases, it can be hypothesized that OM was partly remineralized during (early) diagenesis – lowering TOC values – but (parts of the inventory of) Cu and Ni remained trapped within the sediment. The metals probably remained as sulfides sensu lato (namely, iron sulfides, pyrite or their own sulfides), or accessorily, in the form of tetrapyrroles in the case of Ni. This strongly suggests that OM was remineralized in the presence of sulfide ions in the interstitial waters. In other terms, OM was remineralized through sulfate-reduction reactions, releasing Cu and Ni that were trapped by the by-products of sulfate reduction, namely, sulfide ions.

Here, a specific point is to be discussed. During late diagenesis (cata- and meta-genesis), organic matter could be destroyed by temperature during burial or due to migrations of hot fluids (bringing the OM beyond the oil window or gas window). In such a case, OM would be thermally destroyed but the associated Cu or Ni could have remained trapped in the rocks during the "cooking". In addition, part of the OM could have been turned into hydrocarbons that would have migrate elsewhere. Carbon loss due to maturation and expulsion in a highly mature shale reach ~50% in some occasions (Tissot and Welte, 1984). In such cases, the OM content would have been lowered during late diagenesis long after Cu and Ni had been trapped into pyrite. Therefore, such situations would correspond to a relatively low OM concentration, compared to the Cu-Ni content. Lastly, the formations of the present study with a relative deficit in OM compared to their Cu- and Ni-EF, namely, formations 29, 31, 43, 45, 50 and 52) did not undergo strong burial (Algeo, personal communication and unpublished data, see Tab. 1 and the supplemental reference for the geological background of the formations), which allows the discussion about cata- and meta-genesis to be discarded.

4.3 Influence of sulfate-reduction reactions

Many authors have stressed the importance of sulfate-reduction among the bacterial processes of remineralization of OM (syntheses in Burdige, 2006; Jørgensen, 2006; Rullkötter, 2006; Scholz, 2018 and references therein). This bacterially-mediated sulfate reduction (BSR) may be summarized as:

$$2CH_2O + SO_4^{2-} \xrightarrow{H_2} H_2S + 2HCO_3^-, \qquad (1)$$

and is based on the availability of simple chemical substrates (lactate, butyrate, propionate, H_2). Apart from H_2, these simple substrates are not initially present in large quantities in the interstitial medium, and they are released during the first stages of the decomposition of OM through hydrolysis and enzymatic degradations, or fermentation. If therefore BSR takes place, it is because a certain number of reactions, mainly led by microorganisms, take place beforehand. These reactions consume OM which acts as an electron supplier in redox reactions leading to the reduction of oxides and hydroxides of iron, manganese, or nitrate ions (denitrification). Many works focused on BSR for several reasons: (1) sulfate ions are abundant in seawater and therefore in surface pore waters. The presence of these ions feeds the BSR as long as they are present and/or replenished in interstitial waters. (2) In addition, sulfate reduction results in the release of soluble sulfide ions that can react with any dissolved iron or with OM. It can therefore form iron sulfides (in particular pyrite) or sulfured (a.k.a. vulcanized) OM (Tegelaar *et al.*, 1989; Burdige, 2006; Vandenbroucke and Largeau, 2007; Tribovillard *et al.*, 2015; Findlay *et al.*, 2020).

In the present study, we consider that sulfate reduction operated in each of the situations examined, because this diagenetic step is never omitted in organic-rich marine deposits. As explained in Section 2, for a limited number of formations or sample (sub-) sets (situation 2; formations highlighted in Fig. 4), we interpret a relative deficit in TOC compared to Ni- and Cu-enrichment factors as an evidence of OM remineralization with transfer of Cu and Ni from OM to authigenic phases during the BSR diagenetic step. However a majority of situations show that OM and the Ni-Cu couple were remineralized or released, respectively, without subsequent trapping of the metals in authigenic phases (situation 1). If we consider that BSR is an unavoidable diagenetic step, and that the total absence of OM remineralization cannot be envisaged, the correlations between the enrichments in Cu and Ni and the TOC values, that is, the amount of OM actually present in the sediment, strongly suggest that Cu and Ni released through OM decay have not been retained in the sediment. Therefore, the question is: how is it that sulfate-reduction by-products could not trap Cu and Ni, whereas both elements and, especially, Cu are commonly accumulated during (iron) sulfide precipitation?

4.3.1 Hypothesis 1: iron-limited pyrite precipitation?

A first explanation may come from the possible limitation of Cu and Ni incorporation into pyrite, if the latter precipitates in low abundance. The works examining metal incorporation or adjunction to pyrite (*e.g.*, Huerta-Diaz and Morse, 1992; Berner *et al.*, 2013; Raiswell *et al.*, 2018) underlined the fact that pyrite precipitation may be limited by the availability of reactive iron. In the case where available reactive iron limits or prevents the authigenic precipitation of significant amounts of pyrite, Cu and Ni, being released through OM decay, could be kept in soluble forms in the pore space and then released out of the sediment into the water column. Iron limitation would prevent Cu and Ni fixation. This hypothesis is confirmed by the following observations:

- The formations where TOC and Cu-EF are proportional show Fe:Al ratio values at or close to the average crustal value, that is, without significant authigenic iron enrichment (Figs. 1D–1F and 2).
- The formation with relative deficit in TOC, or, in other words, a relative excess in Cu enrichment, show high Fe:Al values (high enrichment in authigenic iron; Fig. 2A).
- The formations with a relative deficit in Cu enrichment yield Fe:Al ratio values below the crustal value Fig. 2C). To illustrate this situation, two basins reputed for their euxinic conditions, that is, the Cariaco Basin and the Black Sea, may be considered. The samples from the Cariaco Basin do not yield any correlation between TOC and Cu-EF values, contrary to the Black Sea samples (Fig. 1F). Considering their respective Fe:Al ratio, the Cariaco samples show significantly lower values than those of the Black Sea samples (Fig. 4), which strongly suggests that the availability of reactive iron conditioned the way Cu was retained in the sediment. A specific point may be briefly discussed here: the Cariaco Basin shows a high sedimentation rate compared to the Black Sea, and Liu and Algeo (2020) and Crombez *et al.* (2020) recently discussed the fact that a high sedimentation rate can lower the concentrations of some trace metals. The sediment of the Cariaco Basin yield a low arsenic concentration (Tribovillard, 2020) but enrichments in antimony (Tribovillard, unpublished data), although these two metalloids are quite close from a chemical point of view. This discrepancy allows the sedimentation rate to be ruled out as a single factor conditioning trace-element enrichment, in the case of the Cariaco Basin.

4.3.2 Hypothesis 2: Timing of the Cu and Ni release?

Another (possibly complementary) explanation could come from the timing of the various diagenetic steps. If Cu- and Ni release from decaying OM is rapid, that is, takes place during the initial steps (namely, O_2-driven oxidation and denitrification), the metals could be lost from the sediment prior to any capture by iron sulfides, and the iron sulfides would be released too late in the interstitial water to be able to react with Cu and Ni, already gone away. Such a scenario can be envisaged for depositional settings where the redox-cline would be below the sediment-water interface but cannot be considered for euxinic conditions of deposition. In sediments where the redox-cline is below the sediment-water interface, the rapid, bacterially mediated, OM remineralization transforms the initial organic products into bacterial biomass, as underlined by Lehmann *et al.* (2020), which favors Cu- and Ni-release out of the initial organic carrier phase.

In the case of euxinic conditions (H_2S present in the water column), the direct contact between released Cu and Ni and sulfide ions in the seawater would favor rapid metal pyritization, provided sufficient reactive iron is present. An illustration can be provided with two sedimentary formations which were deposited under sulfidic or euxinic conditions, formations 52 and 55 (Hushpuckney Shale), mentioned in the hypothesis 1 above. Figure 5A indeed show that the samples of these formations have marked enrichments both in U and in Mo, which is typical of euxinic conditions (Algeo and Tribovillard, 2009). In other words, sulfide ions were present in the water column when the sediment was deposited. The sulfur contents and the Cu enrichments are high but the two variables are not correlated (Fig. 5B). On the other hand, the Cu enrichments are correlated with the Fe:Al ratio (Fig. 5C), which suggests that the reactive iron must have been the factor limiting the formation of pyrite and, therefore, the trapping of copper.

4.3.3 Hypothesis 3: which type of sulfate reduction?

Another point may have to see with the timing of the sulfate reduction itself. Two types of sulfate reduction may be observed, first, the organoclastic bacterial sulfate reduction (BSR), mentioned above, with micro-organisms using OM as an electron supplier fueling redox reactions where sulfate is reduced into sulfide, and, second, another step of sulfate reduction taking place below the so-called sulfate-methane transition zone (SMTZ; Jørgensen, 2006): the sulfate-dependent anoxic oxidation of methane (AOM) results from a series of reactions involving bacteria and archaea, that can be summarized as:

$$SO_4^{2-} + CH_4 \rightarrow HCO_3^- + HS^- + H_2O. \quad (2)$$

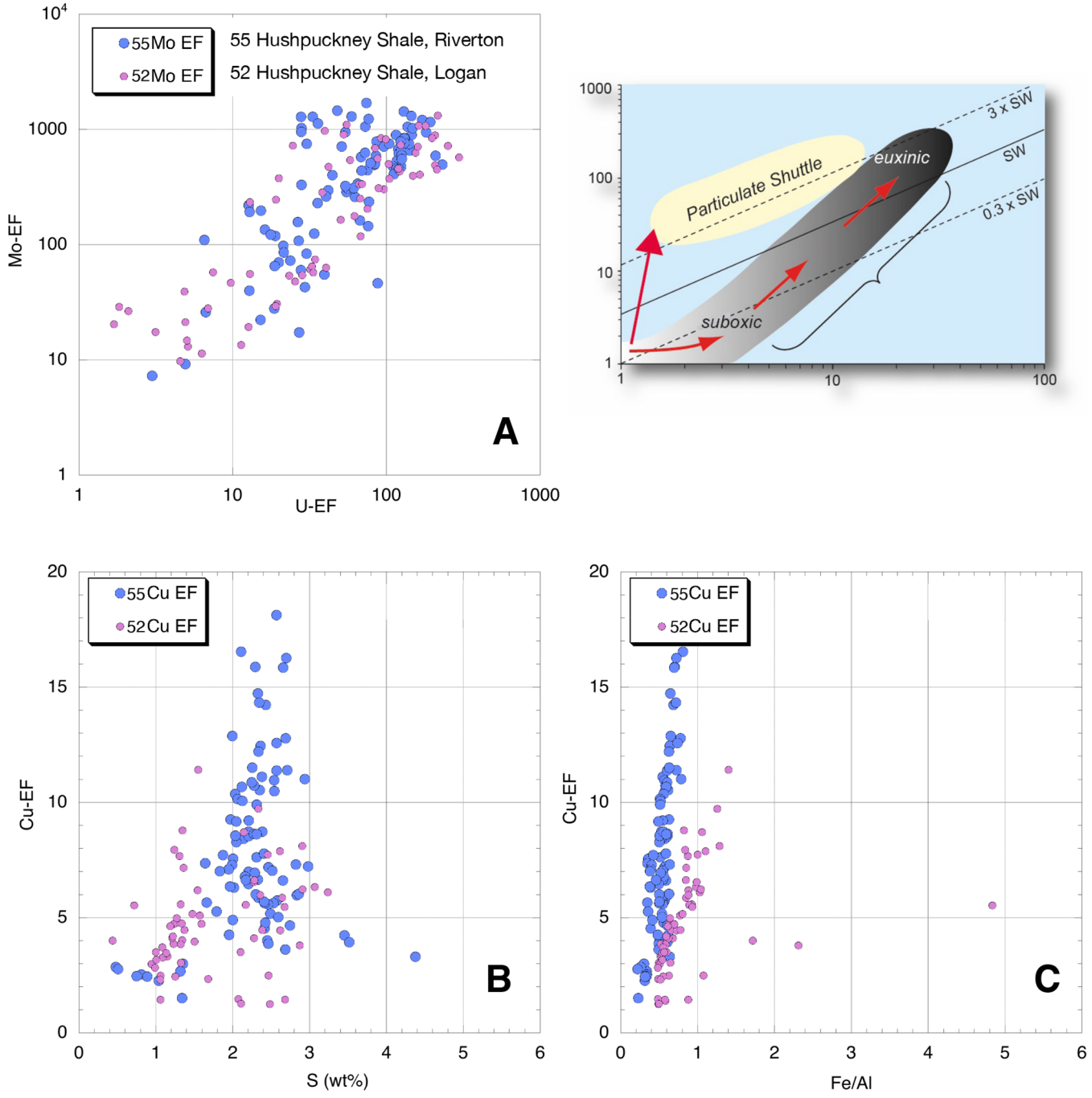

Fig. 5. Cross diagram for the formations 52 and 55, with panel A opposing the enrichment factors in U and Mo, and indicating anoxic-euxinic conditions of deposition (following Algeo and Tribovillard, 2009). Panels B and C show the relations between Cu-EF and the S content (B) or the Fe:Al ratio (C). The formation names are listed in Table 1.

Quijada *et al.* (2016) showed that, in the sediments of the Cariaco Basin, the maximum of H_2S present in interstitial waters was at a certain distance below the sediment-water interface, as a function of the depth of the SMTZ (itself function of the rate of sedimentation, OM flux, etc.). This means that the maximum amount of H_2S will be in contact with an OM that is already buried and therefore already degraded. If this OM is already degraded, it may have lost most of its Cu and Ni content. In other words, the sulfate reduction linked to the AOM stage is too late and less effective in trapping Cu and Ni into sulfides, compared to the more superficial BSR. This organoclastic BSR occurs earlier in the course of diagenesis at a time when Cu and Ni have not yet been fully expelled from the sediment. In addition, the sulfate-dependent AOM involves methane that do not carry metals, whereas the organoclastic sulfate reduction involves organic matter that does carry metals.

An additional difference may come from the fact that the sulfide ions released in the water by the bacterial reactions of

SR can be rapidly re-oxidized, which prevents or considerably limits the formation of metallic sulfides (Rickard, 2012). In modern sediments, Findlay *et al.* (2020) have shown that sulfide oxidation rates in OM-rich, coastal, sediments, were greater than rates of sulfide production through BSR. They calculated up to 92% of BSR-issued sulfide being re-oxidized. The authors showed that Fe oxides were the primary oxidant for sulfide and that the sulfide oxidation rate was related to the amount and reactivity of the Fe-bearing minerals (Findlay *et al.*, 2020).

4.4 Implications for paleo-productivity reconstruction

Reconstructing paleo-productivity levels in marine settings has always been challenging and several approaches have been developed. For instance, many authors developed models based on the sulfur content of the sediments. The BSR, summarized by equation (1) implies that each atom of sulfur, transferred to pyrite or sulfurized OM, corresponds to carbon atoms initially present in the OM before it was remineralized. This simple observation has enabled numerous "stoichiometric" models aiming at restoring the value of the initial TOC (at the time of sedimentation and deposition) from the sulfur content measured today in the sediments (*e.g.*, Littke *et al.*, 1991; Bertrand and Lallier-Vergès, 1993; Vetö *et al.*, 1994; Lückge *et al.*, 1996; Littke *et al.*, 1997). A possible limitation of these models is linked to the actual presence of BSR by-products: pyrite is only present in sediment records if there is sufficient reactive iron present in the interstitial medium at the time of early diagenesis. Sulfurization of OM does not occur automatically and depends on the chemical (molecular) nature of the organic products present at the time of SRB (Aycard *et al.*, 2003; Vandenbroucke and Largeau, 2007; Quijada *et al.*, 2015, 2016; Raven *et al.*, 2016). In other words, since all the sulfur from the BSR is not systematically trapped, this leads to a reduction in the calculated quantity of OM initially present, when the sulfur measured is used to find the degraded OM. A second limitation is linked to the fact that sulfate reduction may also occur as sulfate-dependent AOM (Eq. (2)). In the reaction, only methane molecules are consumed and no other forms of OM. The sulfide ions thus released, if they are recorded in the sediments and measured later, cannot be used to convert sulfur back into organic carbon. Indeed, the methane consumed has several possible origins (bacterial, thermal, with or without migration) and this adds a lot of uncertainty to the modeling.

Alongside this approach, other authors used trace metals to reconstruct past productivity (*e.g.*, François, 1988; Dymond *et al.*, 1992; Brumsack, 2006; Bönning *et al.*, 2015; Little *et al.*, 2015; Sweere *et al.*, 2016). In particular, several works discussed the use of Ni and Cu for paleo-productivity reconstructions (*e.g.*, Shaw *et al.*, 1990; Tribovillard *et al.*, 2006; Piper and Calvert, 2009; Bönning *et al.*, 2015; Steiner *et al.*, 2017). These models are based on the observation of current marine situations showing a good correspondence between productivity and transfer of Ni or Cu to the sediment, as well in contexts of high productivity/low oxygenation (Bönning *et al.*, 2015) as in contexts of low productivity/good oxygenation (Steiner *et al.*, 2017). Furthermore, with regard to ancient sedimentary deposits, Tribovillard *et al.* (2006), Riquier *et al.* (2006, 2010) used the Cu or Ni contents or enrichments as palaeoproductivity markers, considering that these elements are accumulated into the sediments, being brought with OM and that they remain in the host sediments, still linked to the OM, or transferred without loss to pyrite upon OM decay.The present study does not call into question the works cited here, but it obliges us to reconsider the value that can be given to Cu and Ni as markers of paleo-productivity. Our results show that in many cases Cu and Ni are not transferred without loss to pyrite or other iron sulfides during early diagenesis. On the contrary, obviously, it is frequently the case that these metals are lost at the same time, and in the same proportions, as OM. The situations where these metals would suffer the least losses are those where reactive iron does not limit pyritization. In other words, relying on the abundance of Cu or Ni to calculate the initial organic carbon content may lower the result if part of the metal content could not be kept within the sediment. The value of the Fe:Al ratio must be checked; if the ratio is very close, or even lower than the crustal value, it can be anticipated that the result of the calculation of the initial TOC will be too weak.

5 Conclusion

First of all, it should be remembered that, in this study, we were interested in sediments and sedimentary rocks rich, even very rich, in organic matter, which is not the general case of deposits in the marine environment. This paper is intended to be an update on the use that can be made of copper and nickel in paleo-environmental reconstructions. Brought mainly by sedimentary OM, these two metals may not remain trapped in the sediments. Several factors acting on the loss of Cu and Ni can be put forward; among them, let us retain:

- a rapid loss linked to the decomposition of the OM before the conditions conducive to sulfate-reduction set in;
- a low abundance of reactive iron which limits the quantity of pyrite liable to form, which would obviously hamper the possibilities of fixing Cu and Ni.

If Cu and Ni are not reliably retained in the sediments, that is, proportional to the quantity of OM supplied to the sediment, the paleo-environmental reconstitutions involving the concentrations of these metals may provide underestimated values of paleoproductivity. An interesting index to take into account is the Fe:Al ratio that makes it possible to quickly know whether the values of the Cu and Ni enrichments are likely to be "abnormally" low.

The results of this work were obtained from a simple statistical treatment of a large number of data. Such an approach quickly reaches its limits, but it underlines a little further the fact that the paleo-environmental reconstructions must take into account an always larger number of parameters, and that each paleo-setting is be considered as a unique case.

Acknowledgements. I thank Thomas J. Algeo (University of Cincinnati) for his advices and for encouraging me to develop my own ideas and hypotheses from the database he has established over the years and which was published last year in the article by Algeo and Liu (2020). Thanks to the three

reviewers of the manuscript Nicholas Harris, Anthony Chappaz and an anonymous person, for their much appreciated and helpful review. Thanks to the journal's editors Laurent Jolivet and Cécile Robin.

References

Achterberg EP, Van den Berg CMG, Colombo C. 2003. High resolution monitoring of dissolved Cu and Co in coastal surface waters of the western North Sea. *Contin. Shelf Res.* 23: 611–623.

Algeo TJ, Maynard JB. 2004. Trace-element behavior and redox facies in core shales of Upper Pennsylvanian Kansas-type cyclothems. *Chem. Geol.* 206: 289–318.

Algeo TW, Liu J. 2020. A re-assessment of elemental proxies for paleoredox analysis. *Chemical Geology* 540: 119549.

Algeo TJ, Tribovillard N. 2009. Environmental analysis of paleoceanographic systems based on molybdenum-uranium co-variation. *Chemical Geology* 268: 211–225.

Aycard M, Derenne S, Largeau C, Tribovillard N, Baudin F. 2003. Formation pathways of proto-kerogens in Holocene sediments of the upwelling influenced Cariaco Trench, Venezuela. *Org. Geochem.* 34: 701–718.

Berner RA. 1970. Sedimentary pyrite formation. *Am. J. Sci.* 268: 1–23.

Berner RA. 1984. Sedimentary pyrite formation: An update. *Geochim. Cosmochim. Acta* 48: 605–615.

Berner ZA, Puchelt H, Noltner T, Kramar UTZ. 2013. Pyrite geochemistry in the Toarcian Posidonia Shale of south-west Germany: Evidence for contrasting trace element patterns of diagenetic and syngenetic pyrites. *Sedimentology* 60: 548–573.

Bertrand P, Lallier-Vergès E. 1993. Past sedimentary organic matter accumulation and degradation controlled by productivity. *Nature* 364: 786–788.

Bönning P, Shaw T, Pahnke K, Brumsack H-J. 2015. Nickel as indicator of fresh organic matter in upwelling sediments. *Geochimica et Cosmochimica Acta* 162: 99–108.

Bruland KW. 1980. Oceanographic distribution of cadmium, zinc, nickel and copper in the North Pacific. *Earth Planet. Sci. Lett.* 47: 176–198.

Brumsack H-J. 2006. The trace metal content of recent organic carbon-rich sediments: Implications for Cretaceous black shale formation. *Palaeogeogr. Palaeoclimat. Palaeoecol.* 232: 344–361.

Burdige DJ. 2006. Geochemistry of marine sediments. Princeton University Press, 609 p.

Calvert SE, Pedersen TF. 1993. Geochemistry of recent oxic and anoxic sediments: implications for the geological record. *Mar. Geol.* 113: 67–88.

Ciscato ER, Bontognali TRR, Poulton SXW, Vance D. 2019. Copper and its isotopes in organic-rich sediments: from the modern Peru Margin to Archean shales. *Geosciences* 2019(9): 325.

Charriau A, Lesven L, Gao Y, Leermakers M, Baeyens W, Ouddane B, *et al.* 2011. Trace metal behaviour in riverine sediments: Role of organic matter and sulfides. *Applied Geochemistry* 26: 80–90.

Chester R. 1990. Marine Geochemistry. Springer.

Ciscato ER, Bontognali TRR, Vance D. 2018. Nickel and its isotopes in organic-rich sediments: Implications for oceanic budgets and a potential record of ancient seawater. *Earth and Planetary Science Letters* 494: 239–250.

Crombez V, Rohais S, Euzen T, Riquier L, Baudin F, Hernandez-Bilbao E. 2020. Trace metal elements as paleoenvironmental proxies: Why should we account for sedimentation rate variations? *Geology* 48(8): 839–843. https://doi.org/10.1130/G47150.1.

Disnar JR. 1981. Etude expérimentale de la fixation de métaux par un matériau sédimentaire actuel d'origine algaire. *Geochimica et Cosmochimica Acta* 45: 363–379.

Dymond J, Suess E, Lyle. M. 1992. Barium in deep-sea sediments: A geochemical proxy for paleoproductivity. *Paleoceanography* 7: 163–181.

Fernex F, Février G, Benaïm J, Arnoux A. 1992. Copper, lead and zinc trapping in Mediterranean deep-sea sediments: Probable coprecipitation with manganese and iron. *Chem. Geol.* 98: 293–308.

Findlay AJ, Pellerin A, Laufer K, Jørgensen BB. 2020. Quantification of sulphide oxidation rates in marine sediment. *Geochimica et Cosmochimica Acta* 280: 441–452.

François R. 1988. A study on the regulation of the concentrations of some trace metals (Rb, Sr, Zn, Pb, Cu, V, Cr, Ni, Mn and Mo) in Saanich Inlet sediments, British Columbia, Canada. *Mar. Geol.* 83: 285–308.

Giacalone A, Gianguzza A, Orecchio S, Piazzese D, Dongarrà G, Sciarrino S, *et al.* 2005. Metals distribution in the organic and inorganic fractions of soil: A case study on soils from Sicily. *Chemical Speciation & Bioavailability* 17: 83–93.

Gregory DD, Large RR, Halpin JA, Baturina EL, Lyons TW, Wu S, *et al.* 2015. Trace element content of sedimentary pyrite in black shales. *Econ. Geol.* 110(6): 1389–1410.

Grosjean E, Adam P, Connan J, Albrecht P. 2004. Effects of weathering on nickel and vanadyl porphyrins of a Lower Toarcian shale of the Paris basin. *Geochim. Cosmochim. Acta* 68: 789–804

Haraldsson C, Westerlund S. 1988. Trace metals in the water columns of the Black Sea and the Framvaren Fjord. *Mar. Chem.* 23: 417–424.

Huerta-Diaz MA, Morse. JW. 1990. A quantitative method for determination of trace metal concentrations in sedimentary pyrite. *Mar. Chem.* 29: 119–144.

Huerta-Diaz MA, Morse. JW. 1992. Pyritisation of trace metals in anoxic marine sediments. *Geochim. Cosmochim. Acta* 56: 2681–2702.

Jokinen SA, Jilbert T, Tiihonen-Filppula R, Koho K. 2020. Terrestrial organic matter input drives sedimentary trace metal sequestration in a human-impacted boreal estuary. *Science of The Total Environment* 717: 137047.

Jørgensen BB. 2006. Bacteria and marine biogeochemistry. In: Schulz HD, Zabel M, eds. *Marine Geochemistry*, 2nd ed. Springer, pp. 169–201.

Kördel W, Dassenakis M, Lintelmann J, Padberg S. 1997. The importance of natural organic material for environmental processes in waters and soils. *Pure Appl. Chem.* 69: 1571–1600.

Large RR, Halpin JA, Danyushevsky LV, Maslennikov VV, Bull SW, Long JA, *et al.* 2014. Trace element content of sedimentary pyrite as a new proxy for deep-time ocean-atmosphere evolution. *Earth Planet. Sci. Lett.* 389: 209–220.

Large RR, Mukherjee I, Gregory DD, Steadman JA, Maslennikov VV, Meffre S. 2017. Ocean and atmosphere geochemical proxies derived from trace elements in marine pyrite: implications for ore genesis in sedimentary basins. *Econ. Geol.* 112(2): 423–450.

Lehmann MF, Carstens D, Deek A, McCarthy M, Schubert CJ, Zopfi J. 2020. Amino acid and amino sugar compositional changes during in vitro degradation of algal organic matter indicate rapid bacterial re-synthesis. *Geochim. Cosmochim. Acta* 183: 67–84. https://doi.org/10.1016/j.gca.2020.05.025.

Lewan MD, Maynard JB. 1982. Factors controlling enrichment of vanadium and nickel in the bitumen of organic sedimentary rocks. *Geochim. Cosmochim. Acta* 46(12): 2547–2560.

Littke R, Baker DR, Leythaeuser D, Rullkötter J. 1991. Keys to the depositional history of the Posidonia Shale (Toarcian) in the Hils

syncline, northern Germany. In: Tyson RV, Pearson TH, eds. *Modern and ancient continental shelf anoxia*. Geol. Soc. Spec. Publ., vol. 58. The Geological Society, London, pp. 311–334.
Littke R, Lückge A, Welte DH. 1997. Quantification of organic matter degradation by microbial sulphate reduction for Quaternary sediments from the northern Arabian Sea. *Naturwissenschaften* 84: 312–315.
Little SH, Vance D, Lyons TW, McManus J. 2015. Controls on trace metal authigenic enrichment in reducing sediments: insights from modern oxygen-deficient settings. *Am. J. Sci.* 315: 77–119.
Liu J, Algeo TJ. 2020. Beyond redox: Control of trace-metal enrichment in anoxic marine facies by watermass chemistry and sedimentation rate. *Geochim. Cosmochim. Acta* 287: 296–317.
Lückge A, Boussafir M, Lallier-Vergès E, Littke R. 1996. Comparative study of organic matter preservation in immature sediments along the continental margins of Peru and Oman. Part I: Results of petrographical and bulk geochemical data. *Org. Geochem.* 24: 437–451.
McLennan SM. 2001. Relationships between the trace element composition of sedimentary rocks and upper continental crust. *Geochemistry, Geophysics, Geosystems* 2, 2000GC000109.
Marchand C, Fernandez J-M, Moreton B. 2016. Trace metal geochemistry in mangrove sediments and their transfer to mangrove plants (New Caledonia). *Science of the Total Environment* 562: 216–227.
Morel FMM, Milligan AJ, Saito MA. 2003. Marine bioinorganic chemistry: The role of trace metals in the oceanic cycles of major nutrients. In: *Treatise on Geochemistry* (edited by), Vol. 6, pp. 113–143
Morin G, Noël V, Menguy N, Brest J, Baptiste B, Tharaud M, *et al.* 2017. Nickel accelerates pyrite nucleation at ambient temperature. *Geochemical Perspectives Letters* 5: 6–11.
Morse JW, Luther GW. 1999. Chemical influences on trace metal-sulfide interactions in anoxic sediments. *Geochim. Cosmochim. Acta* 63: 3373–3378.
Naimo D, Adamo P, Imperato M, Stanzione D. 2005. Mineralogy and geochemistry of a marine sequence, Gulf of Salerno, *Italy. Quat. Int.* 140-141: 53–63.
Nameroff TJ, Calvert SE, Murray JW. 2004. Glacial–interglacial variability in the eastern tropical North Pacific oxygen minimum zone recorded by redox-sensitive trace metals. *Paleoceanography* 19: PA1010. https://doi.org/10.1029/2003PA000912.
Pedersen TF, Vogel JS, Southon JR. 1986. Copper and manganese in hemipelagic sediments: diagenetic contrasts. *Geochim. Cosmochim. Acta* 50: 2019–2031.
Perkins RB, Piper DZ, Mason CE. 2008. Trace-element budgets in the Ohio/Sunbury shales of Kentucky: Constraints on ocean circulation and primary productivity in the Devonian-Mississippian Appalachian Basin. *Palaeograph. Palaeoclimat. Palaeoecol.* 265: 14–29.
Piper DZ, Perkins RB. 2004. A modern vs. Permian black shale – The hydrography, primary productivity, and water-column chemistry of deposition. *Chemical Geology* 206: 177–197.
Piper DZ, Perkins RB, Rowe HD. 2007. Rare-earth elements in the Permian Phosphoria Formation: paleo proxies of ocean geochemistry. *Deep-Sea Res.* 54: 1396–1413.
Piper DZ, Calvert SE. 2009. A marine biogeochemical perspective on black shale deposition. *Earth Sci. Rev.* 95: 63–96.
Plass A, Dale AW, Scholz F. 2021. Sedimentary cycling and benthic fluxes of manganese, cobalt, nickel, copper, zinc and cadmium in the Peruvian oxygen minimum zone. *Marine Chemistry* 233: 103982.
Poulton SW, Canfield DE. 2011. Ferruginous conditions: A dominant feature of the ocean through Earth's history. *Elements* 7: 107–112.
Raiswell R, Canfield DE. 2012. The iron biogeochemical cycle past and present, *Geochemical Perspectives* 1: 1–220.
Raiswell R, Hardisty DS, Lyons TW, Canfield DE, Owens JD, Planavsky DJ, *et al.* 2018. The iron paleoredox proxies: A guide to the pitfalls, problems and proper practice. *American Journal of Science* 318: 491–526.
Raven MR, Sessions AL, Adkins JF, Thunell RC. 2016. Rapid organic matter sulfurization in sinking particles from the Cariaco Basin water column. *Geochimica et Cosmochimica Acta* 190: 175–190.
Raven MR, Fike DA, Bradley AS, Gomes MS, Owens JD, Webb SA. 2019. Paired organic matter and pyrite δ34S records reveal mechanisms of carbon, sulfur, and iron cycle disruption during Ocean Anoxic Event 2. *Earth and Planetary Science Letters* 512: 27–38.
Rickard D. 2012. Sulfidic sediments and sedimentary rock. Developments in Sedimentology, vol. 65. Elsevier, 801 p.
Riquier L, Tribovillard N, Averbuch O, Devleeschouwer X, Riboulleau A. 2006. The Late Frasnian Kellwasser horizons of the Harz Mountains (Germany): two oxygen-deficient periods resulting from different mechanisms. *Chem. Geol.* 233: 137–155.
Riquier L, Averbuch O, Devleeschouwer X, Tribovillard N. 2010. Diagenetic versus detrital origin of the magnetic susceptibility variations in some carbonate Frasnian-Famennian boundary sections from Northern Africa and Western Europe: Implications for paleoenvironmental reconstructions. *International Journal of Earth Sciences.* 99: S57–S73.
Rullkötter J. 2006. Organic matter: The driving force for early diagenesis. In: Schulz HD, Zabel M, eds. *Marine Geochemistry*, 2nd ed. Springer, pp. 125–162.
Rutten A, de Lange GJ. 2003. Sequential extraction of iron, manganese and related elements in S1 sapropel sediments, eastern Mediterranean. *Palaeogeogr., Palaeoclimat., Palaeoecol.* 190: 79–101.
Quijada M, Riboulleau A, Monnet C, Tribovillard N. 2015. Neutral aldoses derived from sequential acid hydrolysis of sediments as indicators of diagenesis over 120 000 years. *Org. Geochem.* 81: 53–63.
Quijada M, Riboulleau A, Faure P. Michels R, Tribovillard N. 2016. Organic matter sulfurization on protracted diagenetic timescales: the possible role of anaerobic oxidation of methane. *Mar. Geol.* 381: 54–66.
Scholz F. 2018. Identifying oxygen minimum zone-type biogeochemical cycling in Earth history using inorganic geochemical proxies. *Earth-Science Reviews* 184: 29–45.
Sclater FR, Boyle E, Edmond JM. 1976. Marine geochemistry of nickel. *Earth Planet. Sci. Lett.* 31: 119–128.
Shaw TJ, Gieskes JM, Jahnke RA. 1990. Early diagenesis in differing depositional environments: the response of transition metals in pore water. *Geochim. Cosmochim. Acta* 54: 1233–1246.
Steiner Z, Lazar B, Torfstein A, Erez J. 2017. Testing the utility of geochemical proxies for paleoproductivity in oxic sedimentary settings of the Gulf of Aqaba, *Red Sea. Chem. Geol.* 473: 40–49.
Sun Y-Z, Püttmann W. 2000. The role of organic matter during copper enrichment in Kupferschiefer from the Sangerhausen Basin, *Germany. Org. Geochem.* 31: 1143–1161.
Sweere T, van den Boorn S, Dickson AG, Reichart GJ. 2016. Definition of new trace-metal proxies for the controls on organic matter enrichment in marine sediments based on Mn, Co, Mo and Cd concentrations. *Chem. Geol.* 441: 235–245.
Taylor KG, Macquaker JHS. 2011. Iron minerals in marine sediments record chemical environments. *Elements* 7: 113–118.
Tegelaar EW, de Leeuw JW, Derenne S, Largeau C. 1989. A reappraisal of kerogen formation. *Geochim. Cosmochim. Acta* 53: 3103–3106.

Tissot BP, Welte DH. 1984. Petroleum formation and occurrence. 2nd ed. Berlin: Springer-Verlag, 699 pp.
Tribovillard N, Algeo TJ, Lyons TW, Riboulleau A. 2006. Trace metals as paleoredox and paleoproductivity proxies: An update. *Chem. Geol.* 232: 12–32.
Tribovillard N, Bout-Roumazeilles V, Algeo TJ, Lyons TW, Sionneau T, Montero-Serrano JC, *et al.* 2008. Paleodepositional conditions in the Orca Basin as inferred from organic matter and trace metal contents. *Marine Geology* 254: 62–72.
Tribovillard N, Hatem E, Averbuch O, Barbecot F, Bout-Roumazeilles V, Trentesaux A. 2015. Iron availability as a dominant control on the primary composition and diagenetic overprint of organic-matter-rich rocks. *Chemical Geology* 401: 67–82.
Tribovillard N. 2020. Arsenic in marine sediments: How robust a redox proxy? *Palaeogeography, Palaeoclimatology, Palaeoecology* 550: 109745.
Twining BS, Baines SB, Vogt S, Nelson DM. 2012. Role of diatoms in nickel biogeo-chemistry in the ocean. *Global Biogeochem. Cycles* 26: GB4001.
Vandenbroucke M, Largeau C. 2007. Kerogen origin, evolution and structure. *Organic Geochemistry* 38: 719–833.
Van der Weijden CH. 2002. Pitfalls of normalization of marine geochemical data using a common divisor. *Marine Geology* 184: 167–187.
Vetö I, Hetényi M, Demény A, Hertelendi E. 1994. Hydrogen index as reflecting intensity of sulphide diagenesis in nonbioturbated, shaly sediments. *Org. Geochem.* 22: 299–310.
Weng L, Temminghoff EJM, Lofts S, Tipping E, Van Riemsdijk WH. 2002. Complexation with dissolved organic matter and solubility control of heavy metals in a sandy soil. *Environmental Science & Technology* 36: 4804–4810.
Widerlund A. 1996. Early diagenetic remobilization of copper in near-shore marine sediments: a quantitative pore-water model. *Mar. Chem.* 54: 41–53.
Whitfield M. 2002. Interactions between phytoplankton and trace metals in the ocean. *Adv. Mar. Biol.* 41: 3–120.

Supplemental References

References in Table 1 from Algeo and Liu (2020)

Algeo TJ, Li C. 2020. Redox classification and calibration of redox thresholds in sedimentary systems. *Geochimica et Cosmochimica Acta* 287: 8–26. https://doi.org/10.1016/j.gca.2020.01.055.
Algeo TJ, Tribovillard N. 2009. Environmental analysis of paleoceanographic systems based on molybdenum-uranium co-variation. *Chemical Geology* 268(3-4): 211–225.
Algeo TJ, Schwark L, Hower JC. 2004. High-resolution geochemistry and sequence stratigraphy of the Hushpuckney Shale (Swope Formation, eastern Kansas): Implications for climato-environmental dynamics of the Late Pennsylvanian Midcontinent Seaway. *Chemical Geology* 206(3-4): 259–288.
Algeo TJ, Hinnov L, Moser J, Maynard JB, Elswick E, Kuwahara K, *et al.* 2010. Changes in productivity and redox conditions in the Panthalassic Ocean during the latest Permian. *Geology* 38(2): 187–190.
Algeo TJ, Kuwahara K, Sano H, Bates S, Lyons T, Elswick E, *et al.* 2011. Spatial variation in sediment fluxes, redox conditions, and productivity in the Permian-Triassic Panthalassic Ocean. *Palaeogeography, Palaeoclimatology, Palaeoecology* 308(1-2): 65–83.
Brett CE, Baird GC, Bartholomew AJ, DeSantis MK, Ver Straeten CA. 2011. Sequence stratigraphy and a revised sea-level curve for the Middle Devonian of eastern North America. *Palaeogeography, Palaeoclimatology, Palaeoecology* 304(1-2): 21–53.
Brumsack HJ. 1989. Geochemistry of recent TOC-rich sediments from the Gulf of California and the Black Sea. *Geologische Rundschau* 78(3): 851–882.
Cruse AM, Lyons TW. 2004. Trace metal records of regional paleoenvironmental variability in Pennsylvanian (Upper Carboniferous) black shales. *Chemical Geology* 206(3-4): 319–345.
DeSantis MK, Brett CE. 2011. Late Eifelian (Middle Devonian) biocrises: timing and signature of the pre-Kačák Bakoven and Stony Hollow events in eastern North America. *Palaeogeography, Palaeoclimatology, Palaeoecology* 304(1-2): 113–135.
Ellwood BB, Algeo TJ, El Hassani A, Tomkin JH, Rowe HD. 2011. Defining the timing and duration of the Kačák Interval within the Eifelian/Givetian boundary GSSP, Mech Irdane, Morocco, using geochemical and magnetic susceptibility patterns. *Palaeogeography, Palaeoclimatology, Palaeoecology* 304(1-2): 74–84.
François R. 1987, Some aspects of the geochemistry of sulphur and iodine in marine humic substances and transition metal enrichment in anoxic sediments. Ph.D. Dissertation, Univ. of British Columbia, Vancouver, B.C., Canada, 462 pp.
Hatch JR, Leventhal JS. 1992. Relationship between inferred redox potential of the depositional environment and geochemistry of the Upper Pennsylvanian (Missourian) Stark Shale Member of the Dennis Limestone, Wabaunsee County, Kansas, USA. *Chemical Geology* 99(1-3): 65–82.
Henderson CM. 1997. Uppermost Permian conodonts and the Permian-Triassic boundary in the western Canada sedimentary basin. *Bulletin of Canadian Petroleum Geology* 45(4): 693–707.
Herrmann AD, Barrick J, Algeo TJ, Peng Y. 2019. Conodont biofacies and watermass structure of the Middle Pennsylvanian North American Midcontinent Sea. *Palaeogeography, Palaeoclimatology, Palaeoecology*, art. 109235.
Hoffman DL, Algeo TJ, Maynard JB, Joachimski MM, Hower JC, Jaminski J. 1998. Regional and stratigraphic variation in bottomwater anoxia in offshore core shales of Upper Pennsylvanian cyclothems from the Eastern Midcontinent Shelf (Kansas), USA. *Shales and Mudstones* 1: 243–269.
Irino T, Pedersen T. 2000. Geochemical character of glacial to interglacial sediments at Site 1017, southern Californian Margin: Minor and trace elements. *Proc. Ocean Drill. Program Sci. Results* 167: 263–271.
Jaminski J. 1998. Geochemical and petrographic patterns of cyclicity in the Devonian-Mississippian black shales of the central Appalachian Basin. Ph.D. Dissertation, University of Cincinnati, Cincinnati, Ohio, USA, 333 pp.
Jaminski J, Algeo TJ, Maynard JB, Hower JC. 1998. Climatic origin of dm-scale compositional cyclicity in the Cleveland Member of the Ohio Shale (Upper Devonian), Central Appalachian Basin, USA. *Shales and Mudstones* 1: 217–242.
Jones B. 1991. Relationships between organic maturity and inorganic geochemistry in Upper Jurassic petroleum source rocks from the Norwegian North Sea and the United Kingdom. Ph.D. Thesis, University of Newcastle upon Tyne, UK, 410 pp.
Jones B, Manning DAC. 1994, Comparison of geochemical indices used for the interpretation of palaeoredox conditions in ancient mudstones. *Chemical Geology* 111: 111–129.
Krull ES, Lehrmann DJ, Druke D, Kessel B, Yu Y, Li R. 2004. Stable carbon isotope stratigraphy across the Permian-Triassic boundary in shallow marine carbonate platforms, Nanpanjiang Basin, south China. *Palaeogeography, Palaeoclimatology, Palaeoecology* 204 (3-4): 297–315.
Lev SM. 1994. Controls on the preservation of organic carbon in the Middle Ordovician Llanvirn/Llandeilo black shales of southwest

Wales, UK. Master's Thesis, University of Cincinnati, Cincinnati, Ohio, USA.

Luo G, Wang Y, Yang H, Algeo TJ, Kump LR, Huang J, *et al.* 2011. Stepwise and large-magnitude negative shift in δ13Ccarb preceded the main marine mass extinction of the Permian-Triassic crisis interval. *Palaeogeography, Palaeoclimatology, Palaeoecology* 299 (1-2): 70–82.

Lüschen H. 2004. Vergleichende anorganisch-geochemische Untersuchungen an phanerozoischen Corg-reichen Sedimenten: ein Beitrag zur Charakterisierung ihrer Fazies. Ph.D. Dissertation, Universität Oldenburg, Oldenburg, Germany, 186 pp.

Lyons TW. 1992. Comparative study of Holocene Black Sea sediments from oxic and anoxic sites of deposition: Geochemical and sedimentological criteria. Ph.D. Dissertation, Yale University, New Haven, Connecticut, 377 pp.

Lyons TW, Werne JP, Hollander DJ, Murray RW. 2003. Contrasting sulfur geochemistry and Fe/Al and Mo/Al ratios across the last oxic-to-anoxic transition in the Cariaco Basin, Venezuela. *Chemical Geology* 195(1): 131–157.

Murphy AE, Sageman BB, Hollander DJ. 2000. Eutrophication by decoupling of the marine biogeochemical cycles of C, N, and P: A mechanism for the Late Devonian mass extinction. *Geology* 28 (5): 427–430.

Over DJ, Hauf E, Wallace J, Chiarello J, Over JS, Gilleaudeau GJ, *et al.* 2019. Conodont biostratigraphy and magnetic susceptibility of Upper Devonian Chattanooga Shale, eastern United States: Evidence for episodic deposition and disconformities. *Palaeogeography, Palaeoclimatology, Palaeoecology* 524: 137–149.

Piper DZ, Dean WE. 2002. Trace-element deposition in the Cariaco Basin, Venezuela Shelf, under sulfate-reducing conditions: A history of the local hydrography and global climate, 20 ka to the present. *U.S. Geological Survey Prof. Paper 1670*.

Robl TL, Barron LS. 1988. The geochemistry of Devonian black shales in central Kentucky and its relationship to inter-basinal correlation and depositional environment. In: *Devonian of the World: Proceedings of the 2nd International Symposium on the Devonian System*, Canadian Society of Petroleum Geologists Memoir 14, Volume II: Sedimentation, pp. 377–392.

Sageman BB, Murphy AE, Werne JP, Ver Straeten CA, Hollander DJ, Lyons TW. 2003. A tale of shales: the relative roles of production, decomposition, and dilution in the accumulation of organic-rich strata, Middle–Upper Devonian, Appalachian basin. *Chemical Geology* 195(1-4): 229–273.

Schobben M, Stebbins A, Algeo TJ, Strauss H, Leda L, Haas J, *et al.* 2017. Volatile earliest Triassic sulfur cycle: A consequence of persistent low seawater sulfate concentrations and a high sulfur cycle turnover rate?*Palaeogeography, Palaeoclimatology, Palaeoecology* 486: 74–85.

Schoepfer SD, Henderson CM, Garrison GH, Foriel J, Ward PD, Selby D, *et al.* 2013. Termination of a continent-margin upwelling system at the Permian-Triassic boundary (Opal Creek, Alberta, Canada). *Global and Planetary Change* 105: 21–35.

Schoepfer SD, Algeo TJ, Ward PD, Williford KH, Haggart JW. 2016. Testing the limits in a greenhouse ocean: Did low nitrogen availability limit marine productivity during the end-Triassic mass extinction?*Earth and Planetary Science Letters* 451: 138–148.

Shen J, Algeo TJ, Hu Q, Zhang N, Zhou L, Xia W, *et al.* 2012. Negative C-isotope excursions at the Permian-Triassic boundary linked to volcanism. *Geology* 40(11): 963–966.

Shen J, Algeo TJ, Feng Q, Zhou L, Feng L, Zhang N, *et al.* 2013. Volcanically induced environmental change at the Permian-Triassic boundary (Xiakou, Hubei Province, South China): Related to West Siberian coal-field methane releases? *Journal of Asian Earth Sciences* 75: 95–109.

Shen J, Algeo TJ, Chen J, Planavsky NJ, Feng Q, Yu J, *et al.* 2019. Mercury in marine Ordovician/Silurian boundary sections of South China is sulfide-hosted and non-volcanic in origin. *Earth and Planetary Science Letters* 511: 130–140.

Son TH, Koeberl C, Ngoc NL, Huyen DT. 2007. The Permian-Triassic boundary sections in northern Vietnam (Nhi Tao and Lung Cam sections): Carbon-isotope excursion and elemental variations indicate major anoxic event. *Palaeoworld* 16(1-3): 51–66.

Song Y, Gilleaudeau G, Algeo TJ, Over DJ, Anbar A, Xie SC. 2020. Biomarker evidence of algal-microbial community changes linked to redox conditions and enhanced weathering, Upper Devonian Chattanooga Shale. *Geological Society of America Bulletin* 133 (1-2): 409–424. https://doi.org/10.1130/B35543.1.

Tada R, Sato S, Irino T, Matsui H, Kennett JP. 2000. 25. Millennial-scale compositional variations in late quaternary sediments at site 1017, Southern California. In: *Proceedings of the Ocean Drilling Program: Scientific Results*,Vol. 167, pp. 277–296.

Song Y, Gilleaudeau G, Algeo TJ, Over DJ, Anbar A, Xie SC. 2020. Biomarker evidence of algal-microbial community changes linked to redox conditions and enhanced weathering, Upper Devonian Chattanooga Shale. *Geological Society of America Bulletin* 133 (1-2): 409–424. https://doi.org/10.1130/B35543.1.

Turner AC, Algeo TJ, Peng Y, Herrmann AD. 2019. Circulation patterns in the Late Pennsylvanian North American Midcontinent Sea inferred from spatial gradients in sediment chemistry and mineralogy. *Palaeogeography, Palaeoclimatology, Palaeoecology* 531, art. 109023.

Ver Straeten CA, Brett CE, Sageman BB. 2011. Mudrock sequence stratigraphy: a multi-proxy (sedimentological, paleobiological and geochemical) approach, Devonian Appalachian Basin. *Palaeogeography, Palaeoclimatology, Palaeoecology* 304(1-2): 54–73.

Wardlaw BR, Nestell MK, Nestell GP, Ellwood BB, Lan LTP. 2015. Conodont biostratigraphy of the Permian-Triassic boundary sequence at Lung Cam, Vietnam. *Micropaleontology* 61(4): 313–334.

Wignall PB, Newton R. 2003. Contrasting deep-water records from the Upper Permian and Lower Triassic of South Tibet and British Columbia: Evidence for a diachronous mass extinction. *Palaios* 18 (2): 153–167.

Xiong Z, Li T, Algeo T, Nan Q, Zhai B, Lu B. 2012. Paleoproductivity and paleoredox conditions during late Pleistocene accumulation of laminated diatom mats in the tropical West Pacific. *Chemical Geology* 334: 77–91.

Zhang L, Orchard MJ, Algeo TJ, Chen ZQ, Lyu Z, Zhao L, *et al.* 2019. An intercalibrated Triassic conodont succession and carbonate carbon isotope profile, Kamura, Japan. *Palaeogeography, Palaeoclimatology, Palaeoecology* 519: 65–83.

Cite this article as: Tribovillard N. 2021. Re-assessing copper and nickel enrichments as paleo-productivity proxies, *BSGF - Earth Sciences Bulletin* 192: 54.